Thermally irreversible supramolecular hydrogels record thermal history

Tominaga, Yudai ; Kanemitsu, Sayuki ; Yamamoto, Shota ; Kimura, Toshihisa ; Nishida, Yuki ; Morita, Kenta ; Maruyama, Tatsuo

(Citation)
Colloids and Surfaces A: Physicochemical and Engineering Aspects,656:130416

(Issue Date)
2023-01-05

(Resource Type)
journal article

(Version)
Accepted Manuscript

(URL)
https://hdl.handle.net/20.500.14094/0100480892

Thermally irreversible supramolecular hydrogels record thermal history

Yudai Tominaga,[a] Sayuki Kanemitsu,[a] Shota Yamamoto,[a] Toshihisa Kimura,[a] Yuki Nishida,[a] Kenta Morita,[a] and Tatsuo Maruyama[a,b]*

[a]Department of Chemical Science and Engineering, Graduate School of Engineering, Kobe University, 1-1 Rokkodai, Nada-ku, Kobe 657-8501, Japan.

[b]Research Center for Membrane and Film Technology, Kobe University, 1-1 Rokkodai, Nada-ku, Kobe 657-8501, Japan.

KEYWORDS: hydrogel, peptide amphiphile, phase diagram, self-assembly, Schiff base, visual detection

*Corresponding author

tmarutcm@crystal.kobe-u.ac.jp

Abstract

A low-molecular-weight gelator produces a supramolecular hydrogel, which shows thermoreversible gel-sol transition. Here, we first report a thermo-"irreversible" hydrogel constructed from a novel low-molecular-weight gelator using dynamic covalent chemistry and its application to thermal history recording. The low-molecular-weight gelator, which was composed of a peptide, an alkyl chain and an aromatic ring, was synthesized via the Schiff base formation using a volatile aromatic aldehyde and an amine-terminated peptide amphiphile. The prepared hydrogel underwent gel-to-sol transition upon heating, which was similar to other reported supramolecular hydrogels. Interestingly, the resultant sol did not return to the gel state upon cooling under designed conditions, indicative of a thermo-irreversible hydrogel. We also demonstrated that thermo-irreversible hydrogels record thermal history without requiring electrical power for applications in logistics.

1. Introduction

Supramolecular hydrogels have attracted broad attention as functional soft materials owing to their designable functions and stimuli-responsiveness [1-3]. They include low-molecular-weight gels [4, 5], polymer-based gels [6], inorganic-based gels, and hybrid gels [7, 8]. In the last two decades, there have been numerous studies on low-molecular-weight hydrogels, ranging from the development of novel low-molecular-weight gelators (LMWGs) to applications of the resultant hydrogels [5, 9, 10]. Molecules of LMWGs self-assemble to form entangled or branched nanofibers (or nanosheets) through noncovalent forces (e.g., H-bonding, π–π stacking, van der Waals interactions) in a solvent. The three-dimensional network of the self-assembly entraps a large amount of water (or an organic solvent), leading to hydrogelation (or organogelation). Among LMWGs developed for the formation of hydrogels, amino acid-based amphiphilic LMWGs (often called peptide amphiphiles) are relatively easy to synthesize and, importantly, can be used to produce precisely designed hydrogels that are responsive to various external stimuli (e.g., heat, pH, light, enzymes, and redox conditions) [11-13]. For molecular self-assembly, the amide bonds and hydrophobic moieties in peptide amphiphiles participate in H-bonding and hydrophobic interactions, respectively. One of the major characteristics of low-molecular-weight hydrogels is thermo-reversible gel–sol transition [14-17]. In general, low-molecular-weight hydrogels transform into the sol upon heating, and the sol turns into the gel upon cooling. Unlike previous low-molecular-weight hydrogels, we here developed a thermo-*irreversible* hydrogel capable of recording thermal history from a novel LMWG using dynamic

covalent bonding and a volatile aldehyde. To the best of our knowledge, this is the first report on a thermo-irreversible hydrogel prepared using a LMWG.

2. Experimental

2.1. Materials

Fmoc-Gly-OH, 12-(Fmoc-amino)dodecanoic acid (Fmoc-Adod(12)-OH), H-His(Trt)-Trt(2-Cl)-resin, 2-(1H-benzotriazole-1-yl)-1,1,3,3-tetramethyluronium hexafluorophosphate (HBTU), 1-hydroxybenzotriazole hydrate (HOBT·H_2O), triisopropylsilane (TIPS), and *N*,*N*-dimethylformamide (DMF) were purchased from Watanabe Chemical Industry (Hiroshima, Japan). Dimethyl sulfoxide (DMSO), *N,N*-diisopropylethylamine (DIEA), benzaldehyde, p-tolualdehyde, 4-ethylbenzaldehyde (EBAL), cyclohexanecarboxaldehyde, propionaldehyde, *n*-butyraldehyde, valeraldehyde , 1-hexanal, and sinapinic acid (SA) were purchased from Tokyo Chemical Industry (Tokyo, Japan). Other chemicals were purchased from Fujifilm Wako Pure Chemical Corporation (Osaka, Japan). High-quality deionized water (DI water, >15 MΩ·cm) produced by an Elix-5 system (Millipore, Molsheim, France) was used in the experiments.

2.2. Solid-phase synthesis of NH_2-C12-G_3H

NH_2-C12-G_3H (NH_2-C12-Gly-Gly-Gly-His) was synthesized by standard 9-fluorenylmethoxycarbonyl (Fmoc) solid-phase peptide synthesis on a 0.6-mmol scale. H-His(Trt)-

Trt(2-Cl)-resin was used as the polymeric support. Fmoc-Gly-OH (3 equiv.) was coupled to the resin (0.6 mmol) using HBTU and HOBT·H_2O as coupling agents in the presence of DIEA in DMF for 60 min at room temperature. Fmoc-Adod(12)-OH (3 equiv.) was coupled to the N-terminus of the synthesized peptide using the coupling agents in the presence of DIEA in DMF for 90 min at room temperature. A coupling reaction in each step was confirmed by the Kaiser test. After each coupling reaction, the Fmoc groups were removed by mixing with a piperidine/DMF (20/80) mixture for 45 min at room temperature. Removal and cleavage of the synthesized peptides from the resin were performed in a mixture of TFA, TIPS, and water at a volume ratio of 95:2.5:2.5 for 90 min at room temperature. The synthesized peptides in the cleavage mixture were precipitated with diethyl ether, collected by centrifugation, washed three times with diethyl ether, and freeze-dried.

An HPLC system (LC-20AT, Shimadzu, Kyoto, Japan) equipped with an Inertsil ODS-3 column (10 × 250 mm, GL Science, Tokyo, Japan) was used to purify the synthesized peptides. The mobile phase was a mixture of water containing TFA (0.1 wt%) and acetonitrile containing TFA (0.1 wt%), and the flow rate was 5 mL/min. The eluted compounds were characterized by measuring the absorbance at 230 nm. The gradient started at 0% acetonitrile and 100% water, and the proportion of acetonitrile was increased to 40% over 8 min. Isocratic 40% acetonitrile was maintained for 2 min. The purified product was freeze-dried and obtained as a dry white powder in 30% to 40% yield. The obtained product was identified by matrix-assisted laser desorption ionization time-of-flight mass spectrometry (MALDI–TOF/MS) using an UltrafleXtreme^{TM} mass spectrometer (Bruker, Billerica,

MA, USA) and sinapinic acid as the matrix. MALDI–TOF/MS (*m/z*) for $[M+H]^+$ of $C_{24}H_{41}N_7O_6$, was 524.2 (calculated: 523.31).

2.3. Synthesis of supramolecular gelator

4-Ethylbenzaldehyde (EBAL) (8.0 mmol) in DMSO was added to a glass tube (inner diameter: 8 mm) containing NH_2-C12-G_3H (8.0 mmol) in bicarbonate buffer solution (pH 10.0, 50 mM, 500 μL). The sum of the concentrations of two compounds was 1 wt%. After it was mixed well, the solution was kept for approximately 1 h at room temperature without stirring. After 1 h, gelation was confirmed by inversion of the glass tube containing the solution. Synthesis of the supramolecular gelator was confirmed by MALDI–TOF/MS (UltrafleXtreme, Bruker, Billerica, MA) using sinapinic acid as the matrix. *m/z* for $[M+H]^+$ of $C_{33}H_{50}N_7O_6$ was 640.4 (calculated: 640.38).

2.4. Transmission electron microscopy (TEM) observation

Transmission electron microscopy (TEM) measurements were carried out using a transmission electron microscope (JEOL2100F, JEOL, Tokyo, Japan). A piece of the gel (1 wt%) was placed on a carbon-coated copper grid and stained with phosphotungstic acid (1 wt%). The grid was dried overnight under vacuum and observed at an acceleration voltage of 200 kV.

2.5. Gas chromatography (GC) analysis

A gas chromatography (GC, GC-2014, Shimadzu, Kyoto, Japan) machine equipped with a flame ionization detector and an InertCap WAX capillary column (30 m × 0.32 mm i.d., 0.50 μm film thickness, GL Sciences, Tokyo, Japan) was used to quantify the EBAL concentration. The gas chromatographic oven temperature was held at 200 °C for 10 min. The linear velocity of the helium carrier gas flow was 26.5 cm/s, and the injector and detector temperatures were 255 °C.

2.6. Heating gel samples in a sand bath

A heating experiment of the gel in a glass tube (volume of 8 mL) was carried out using a thermostatic sand bath with a thermometer. For irreversible gel–sol transition, the lid of the sample was opened during heating. After heating, it was left at room temperature with the lid closed for 24 h.

2.7. Quantification of EBAL and NH_2-C12-G_3H after heating

After heating the gel sample, the NH_2--C12-G_3H concentration was determined by weight change of the sample, which was derived from water evaporation. The EBAL concentration was determined using ^{1}H-NMR spectroscopy.

2.8. Rheological measurements

Rheological measurements were carried out using a rheometer (Anton Paar Physica MCR301, Graz,

Austria) with a parallel plate (diameter of 5.0 cm) at a strain of 0.1% and a gap of 0.3 mm. A mixture composed of 8 mM NH_2-C12-G_3H and 8 mM *p*-tolualdehyde at pH 10.0 was loaded on a sample plate for the measurements.

3. Results and discussion

3.1. Hydrogel formation and its characterization

We designed and synthesized the precursor, a peptide amphiphile of the sequence NH_2-C12-Gly-Gly-Gly-His (NH_2-C12-G_3H), by the standard Fmoc solid-phase peptide synthesis method (Fig. S1 & S2) [18]. We adopted the Schiff base formation for dynamic covalent bonding, wherein NH_2-C12-G_3H forms a Schiff base by reacting with various aldehydes (Fig. 1a & b). We conjectured that the resultant compounds self-assemble to form nanofibers via H-bonding and hydrophobic interactions, resulting in hydrogelation [16]. Eight different aldehydes were used for the reaction in an aqueous buffer at various pH values. A few samples turned into transparent or opaque hydrogels (Fig. 1c) 24 h after the aldehyde and NH_2-C12-G_3H were mixed in a buffer at room temperature. In particular, three different aldehydes with aromatic rings produced hydrogels after mixing with NH_2-C12-G_3H at pH 10.0. Two of these aldehydes also produced hydrogels at pH 7.4 but not at acidic pH. For example, a hydrogel was successfully prepared using 8 mM NH_2-C12-G_3H and 8 mM *p*-tolualdehyde at pH 10.0. The storage modulus (*G'*) of the hydrogel was significantly higher than the loss modulus (*G"*) from the beginning of mixing (Fig. 2a), which was typical of a gel. Aldehydes with linear and cyclic alkyl chains

did not produce hydrogels after mixing with NH_2-C12-G_3H irrespective of the pH.

McCormick et al. reported the successful formation of a Schiff base on a polymer at alkaline pH and its hydrolysis at acidic pH [20], which is consistent with our present results. Among the various conditions tested, mixing 8 mM 4-ethylbenzaldehyde (EBAL) and 8 mM NH_2-C_{12}-G_3H at pH 10.0 produced a hydrogel, which was determined visually as a gel by tilting the solution (Fig 1c). In the following experiments, we adopted these conditions as standard reaction conditions.

a

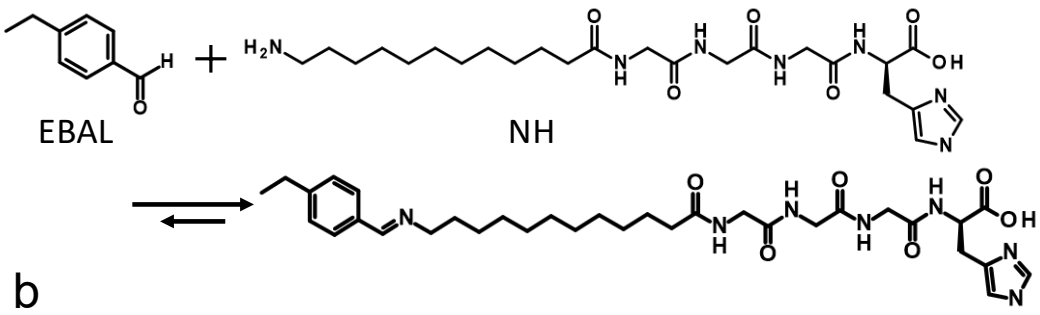

b

Aldehyde (b.p. °C)	pH 4.0	pH 7.4	pH 10.0
(178.1)	Sol	TG	TG
(205)	Sol	TG	OG
(221)	Sol	Sol	OG
(161~163)	Sol	Sol	Sol
(48.8)	Sol	Sol	Sol
(74.8)	Sol	Sol	Sol
(103)	Sol	Sol	Sol
(129)	Sol	Aggregate	Sol

c

Fig. 1 (a) Reaction of 4-ethylbenzaldehyde (EBAL) with NH_2-C12-G_3H to produce a supramolecular gelator (gelator 1). (b) Results of gelation experiments using various aldehydes and NH_2-C12-G_3H at

pH 4.0, 7.4, and 10.0. In each case, equimolar amounts of the aldehyde and NH_2-C12-G_3H were used, and the sum of the two components was 0.5 wt%. TG and OG represent the transparent gel and opaque gel, respectively. (c) Photo of the hydrogel prepared using 8 mM NH_2-C12-G_3H and 8 mM EBAL at pH 10.0 in a glass vial.

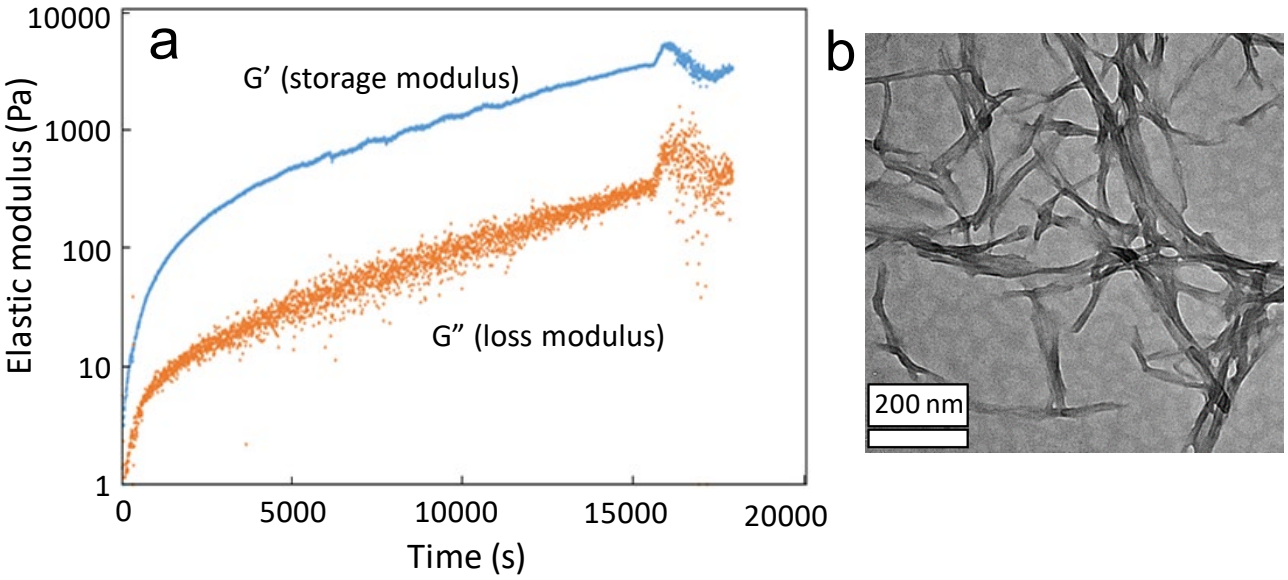

Fig. 2 a) Rheological properties of the hydrogel prepared with 8 mM NH_2-C12-G_3H and 8 mM *p*-tolualdehyde at pH 10.0. b) TEM image of the xerogel prepared using 8 mM NH_2-C12-G_3H and 8 mM EBAL at pH 10.0.

To confirm the synthesis of the supramolecular hydrogelator (gelator 1) consisting of NH_2-C12-G_3H and EBAL, MALDI-TOF/MS measurements were conducted (Fig. S3). The peak at m/z 640.4 indicated the successful synthesis of gelator 1. Gas chromatography measurements revealed that 11% EBAL was consumed in the reaction with NH_2-C12-G_3H, which also supported successful synthesis.

The transmission electron microscopy (TEM) image of the hydrogel showed that there was a fibrous

network and that the strip-like nanofibers were approximately 10 to 50 nm in width, which originated in the self-assembly of the gelator molecules produced (Fig. 2b). In general, the thicker the nanofibers are, the more opaque the gel becomes. The thin nanofibers would account for the transparency of the hydrogel. The above gas chromatography measurements revealed that only 11 % of NH_2-C12-G_3H was converted to gelator **1**. The final concentration of gelator **1** was estimated to be approx. 1 mM (0.064 wt%). This low concentration suggested that NH_2-C12-G_3H and gelator **1** co-assembled to form nanofibers that contributed to the hydrogelation. [21]

Figure S4 shows the magnified ^{1}H-NMR spectra of NH_2-C12-G_3H and the hydrogelator (gelator **1**). Because an imidazole ring has an aromatic property, His residues can produce π–π interaction. The =CH– signal for H_6 in a His residue was slightly shifted upfield (a red arrow in Fig. S4), which indicates the π–π interaction [19]. The addition of 2 M urea turned the hydrogel to a sol, implying hydrophobic interactions in the self-assembly. These results suggested that the π–π interaction and hydrophobic interactions participated in intermolecular interactions in the produced molecules, leading to hydrogelation.

Stored in a glass vial with a tightly closed lid at room temperature, the hydrogel remained in the gel state for more than 4 weeks, indicating long-term stability. DSC measurements of the hydrogel showed an endotherm from approximately 40 °C during heating (Fig. 3a). Indeed, it showed reversible gel–sol transition when it was heated to 40 °C, maintained at that temperature, and then cooled to 25 °C (Fig. 3b).

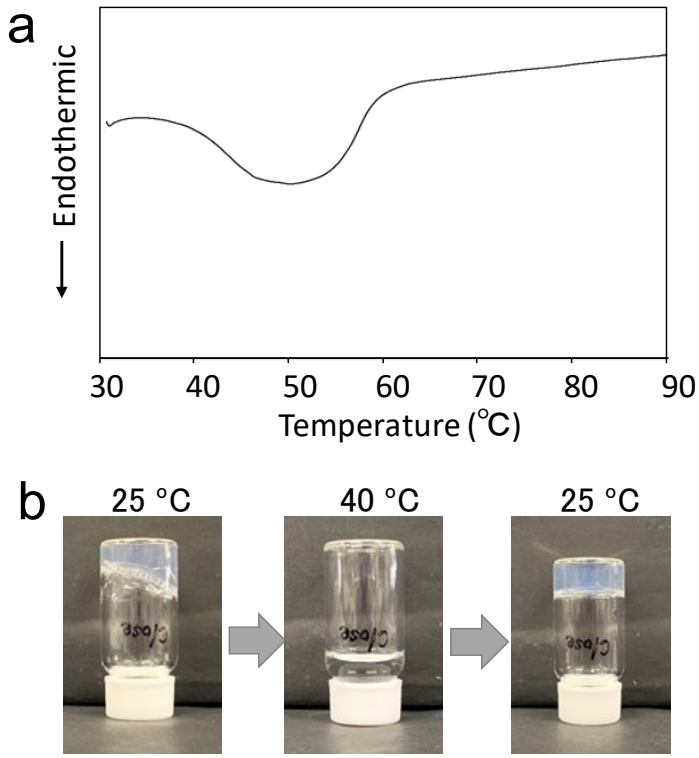

Fig. 3 a) Differential scanning calorimetry analysis of the hydrogel prepared with 8 mM NH_2-C12-G_3H and 8 mM EBAL at pH 10.0. Heating rate was 1 °C/min. b) Reversible gel–sol transition of the hydrogel in a glass vial with a tightly closed lid. The hydrogel was prepared with 8 mM NH_2-C12-G_3H and 8 mM EBAL at pH 10.0.

3.2. Thermo-irreversible gel–sol transition

To investigate the thermo-irreversible gel–sol transition of the hydrogel, we carried out gel–sol transition experiments using a glass vial with the lid open (Fig. 4). The sample was heated to 80 °C and maintained at that temperature for 40 min with the lid open and then cooled to room temperature, at which point the lid was put on the vial. The sample did not turn into a hydrogel even after it was left for 3 days. We hypothesized that thermo-irreversible gel–sol transition occurred as follows. A part of EBAL in the sample evaporated during heating, and the equilibrium of the reaction (Fig. 1a) shifted to

the left, which reduced the amount of gelator molecules, thus preventing gelation. To test our hypothesis, we prepared a gel–sol phase diagram. NH_2-C12-G_3H and EBAL were mixed at 80 °C under systematically varied concentration conditions to produce the gel–sol phase diagram (Fig. 5a). Mixing EBAL and NH_2-C12-G_3H at high concentrations resulted in gelation (blue diamonds in Fig. 5a), and mixing these components at low concentrations produced a sol (red circles in Fig. 5a). At intermediate concentrations, a viscous solution was produced (green triangles in Fig. 5a). This phase diagram indicated that thermo-irreversibility of the gel–sol transition originated in the evaporation of EBAL.

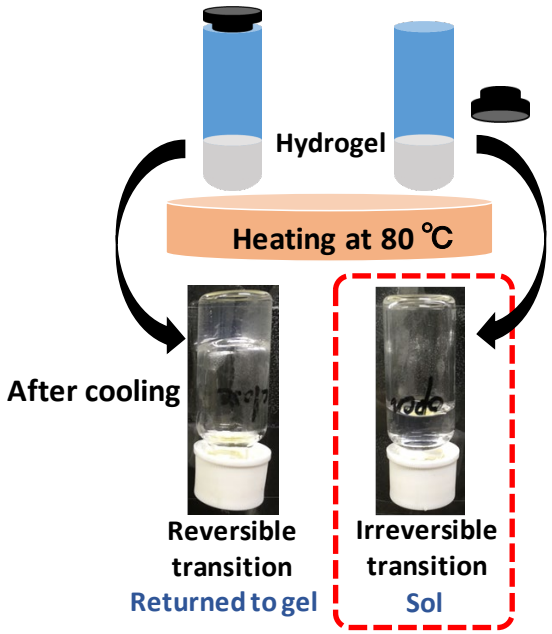

Fig. 4 Photos of hydrogel samples after heating and cooling in a glass vial with and without a tightly closed lid. The hydrogel was prepared using a mixture of NH_2-C12-G_3H and EBAL (8 mM each) at pH 10.0.

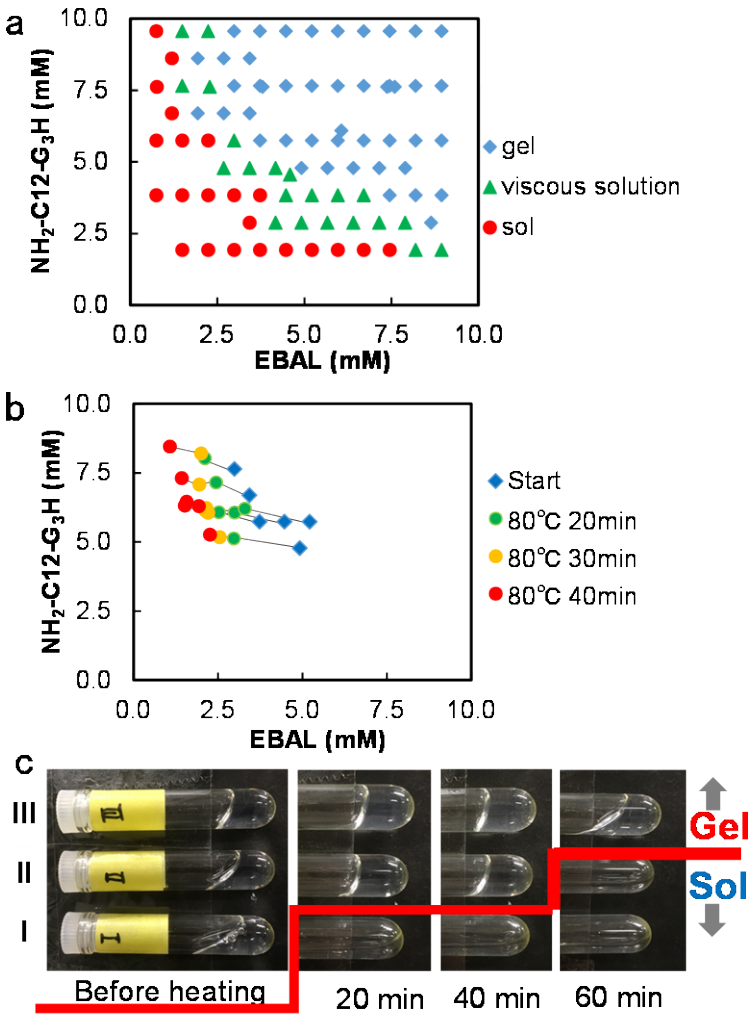

Fig. 5 a) Gel–sol phase diagram of a mixture of EBAL and NH_2-C12-G_3H at pH 10.0. The state of the sample (gel, viscous solution, or sol) was determined by tilting the glass vial containing the mixture solution. b) NH_2-C12-G_3H and EBAL concentrations before and after heat treatment at 80 °C for given periods. c) Photos of hydrogel samples after heat treatment at 80 °C for given periods and cooling to room temperature. After heat treatment at 80 °C and cooling to room temperature, samples above the red line were gels, while those below the red line were in the sol state. Determination of the sample state (gel, viscous solution, or sol) was carried out 24 h after cooling to room temperature. The EBAL concentration of sample I, II, and III were 3.7 mM, 6.0 mM,

and 8.2 mM, respectively. The NH_2-C12-G_3H concentration was set to 5.7 mM for all samples.

To discuss the thermo-irreversible process quantitatively, ^{1}H-NMR measurements were performed to quantitate the EBAL concentration before and after the heat treatment. Evaporation of water during the heat treatment was also evaluated by weighing the sample. We prepared hydrogel samples at six different concentration conditions (EBAL and NH_2-C12-G_3H) and kept them at 80 °C for various periods with the lid open. The EBAL concentration decreased with the heating period, and a small amount of water evaporated, represented as coordinated movement in Fig. 5b (from the gel-to-sol region). For instance, when 5 mM EBAL solution was used, 35% of EBAL evaporated during the heating at 80 °C for 20 min. These samples turned into a sol and retained the sol state after they were maintained at 80 °C for 40 min and kept at room temperature for more than 24 h, which was consistent with the phase diagram. We also subjected the hydrogel samples (with the lid open) to heat treatment at 70 °C and 60 °C. Fig. S5 also shows coordinated movements in the phase diagram from right to left. Because the movements in the phase diagram were derived mainly from EBAL evaporation, the magnitudes of the movements depended on the heating temperature and time.

Finally, we applied this thermo-irreversible supramolecular hydrogel to record thermal history. The hydrogel samples were prepared in glass vials with the lid open using 5.7 mM NH_2-C12-G_3H and EBAL at three different concentrations. All samples were gels before the heat treatment. These hydrogel samples were maintained at 80 °C for given periods and then kept at room temperature for

24 h with the lid off. When sample I (containing 3.7 mM EBAL) was maintained at 80 °C for 20, 40, and 60 min, it turned into a sol and remained a sol even at 24 h after cooling to room temperature (Fig. 5c). In the case of sample II (containing 6.0 mM EBAL), the sample maintained at 80 °C for 60 min remained a sol and the samples maintained at 80 °C for 20 and 40 min recovered to the gel state 24 h after cooling to room temperature. When sample III (containing 8.2 mM EBAL) was heated in a similar fashion, it recovered to the gel state regardless of the heating periods. These results indicated that the heating period at 80 °C was recorded and visualized as the gel or sol state. The recording and visualization of thermal history was also studied at 50 °C and was achieved using EBAL at fine-tuned concentrations (Fig. S6).

4. Conclusion

In the present study, we first succeeded in the preparation of thermo-*irreversible* supramolecular hydrogels using dynamic covalent bonding. Thermo-irreversibility of the LMWG molecule was designed using Schiff-base formation and a volatile aldehyde. Thermo-irreversible hydrogels (in a vial with the lid open) showed gel-to-sol transition upon heating and the resultant sol did not return to the gel state upon cooling. Controlling the concentration of the LMWG component resulted in an irreversible gel-to-sol transition depending on the thermal history (temperature and time), which was determined visually. In this century, logistics and storage of heat-sensitive products (e.g., agricultural products, food, drugs, and electronic devices) are increasing important in the world [22-24]. Although

temperature control during the transportation and storage of those products is vital, it is often hard to monitor or record the thermal history. The present study proposes that thermo-irreversibility supramolecular chemistry would facilitate the development of novel supramolecular devices for recording thermal history without requiring electrical power to support our modern society.

CRediT authorship contribution statement

Y. Tominaga performed the most of experiments and writing a draft. S. Kanemitsu and T. Kimura checked the reproducibility. S. Yamamoto provided and instructed the methodology and the synthesis. Y. Nishida found the phenomena. T. Kimura and K. Morita did ^{1}H-NMR measurements and analysis. Maruyama designed and directed the project.

Declaration of Competing Interest

The authors declare no competing financial interest.

Data Availability

Data will be made available on request.

Acknowledgments

This study was financially supported by Takeda Science Foundation, The Uehara Memorial Foundation, and by JSPS KAKENHI Grant Numbers 19H05458, 20H02542, 21K18850 and

20H04711. The authors thank Prof. A. Kondo and Prof. H. Minami for their technical help with MALDI-TOF/MS and DSC. The authors thank Edanz (https://jp.edanz.com/ac) for editing a draft of this manuscript.

Appendix A. Supplementary material: Supplementary data associated with this article can be found in the online version at doi

References

[1] X. Du, J. Zhou, J. Shi, B. Xu, Supramolecular Hydrogelators and Hydrogels: From Soft Matter to Molecular Biomaterials, Chem Rev, 115 (2015) 13165-13307.
[2] J. Omar, D. Ponsford, C.A. Dreiss, T.C. Lee, X.J. Loh, Supramolecular Hydrogels: Design Strategies and Contemporary Biomedical Applications, Chem. Asian J., 17 (2022).
[3] Z.W. Hao, H.K. Li, Y. Wang, Y.K. Hu, T.H. Chen, S.W. Zhang, X.D. Guo, L. Cai, J.F. Li, Supramolecular Peptide Nanofiber Hydrogels for Bone Tissue Engineering: From Multihierarchical Fabrications to Comprehensive Applications, Adv. Sci., 9 (2022).
[4] K. Hanabusa, M. Suzuki, Physical Gelation by Low-Molecular-Weight Compounds and Development of Gelators, Bull. Chem. Soc. Jpn., 89 (2016) 174-182.
[5] E.R. Draper, D.J. Adams, Low-Molecular-Weight Gels: The State of the Art, Chem, 3 (2017) 390-410.
[6] E.A. Appel, J. del Barrio, X.J. Loh, O.A. Scherman, Supramolecular polymeric hydrogels, Chem. Soc. Rev., 41 (2012) 6195-6214.
[7] T. Montheil, C. Echalier, J. Martinez, G. Subra, A. Mehdi, Inorganic polymerization: an attractive route to biocompatible hybrid hydrogels, Journal of Materials Chemistry B, 6 (2018) 3434-3448.
[8] Y. Eguchi, T. Kato, T. Tanaka, T. Maruyama, A DNA-gold nanoparticle hybrid hydrogel network prepared by enzymatic reaction, Chem. Commun., 53 (2017) 5802-5805.
[9] L.M. De Leon Rodriguez, Y. Hemar, J. Cornish, M.A. Brimble, Structure-mechanical property correlations of hydrogel forming beta-sheet peptides, Chem. Soc. Rev., 45 (2016) 4797-4824.
[10] T. Giraud, P. Hoschtettler, G. Pickaert, M.C. Averlant-Petit, L. Stefan, Emerging low-molecular weight nucleopeptide-based hydrogels: state of the art, applications, challenges and perspectives, Nanoscale, 14 (2022) 4908-4921.
[11] M. Vazquez-Gonzalez, I. Willner, Stimuli-Responsive Biomolecule-Based Hydrogels and Their Applications, Angew. Chem. Int. Ed., 59 (2020) 15342-15377.
[12] S. Panja, D.J. Adams, Stimuli responsive dynamic transformations in supramolecular gels, Chem. Soc. Rev., 50 (2021) 5165-5200.

[13] W.W. Han, W. Xiang, Q.Y. Li, H.W. Zhang, Y.B. Yang, J. Shi, Y. Ji, S.C. Wang, X.F. Ji, N.M. Khashab, J.L. Sessler, Water compatible supramolecular polymers: recent progress, Chem. Soc. Rev., 50 (2021) 10025-10043.
[14] S. Roy, A. Dasgupta, P.K. Das, Alkyl chain length dependent hydrogelation of L-tryptophan-based amphiphile, Langmuir, 23 (2007) 11769-11776.
[15] A. Ghosh, J. Dey, pH-Responsive and Thermoreversible Hydrogels of N-(2-hydroxyalkyl)-L-valine Amphiphiles, Langmuir, 25 (2009) 8466-8472.
[16] D. Koda, T. Maruyama, N. Minakuchi, K. Nakashima, M. Goto, Proteinase-mediated drastic morphological change of peptide-amphiphile to induce supramolecular hydrogelation, Chem. Commun., 46 (2010) 979-981.
[17] N. Minakuchi, K. Hoe, D. Yamaki, S. Ten-No, K. Nakashima, M. Goto, M. Mizuhata, T. Maruyama, Versatile supramolecular gelators that can harden water, organic solvents and ionic liquids, Langmuir, 28 (2012) 9259-9266.
[18] Y. Nishida, A. Tanaka, S. Yamamoto, Y. Tominaga, N. Kunikata, M. Mizuhata, T. Maruyama, In Situ Synthesis of a Supramolecular Hydrogelator at an Oil/Water Interface for Stabilization and Stimuli-Induced Fusion of Microdroplets, Angew. Chem. Int. Ed., 56 (2017) 9410-9414.
[19] F. Allix, P. Curcio, N.P. Quoc, G. Pickaert, B. Jamart-Gregoire, Evidence of Intercolumnar pi-pi Stacking Interactions in Amino-Acid-Based Low-Molecular-Weight Organogels, Langmuir, 26 (2010) 16818-16827.
[20] X.W. Xu, J.D. Flores, C.L. McCormick, Reversible Imine Shell Cross-Linked Micelles from Aqueous RAFT-Synthesized Thermoresponsive Triblock Copolymers as Potential Nanocarriers for "pH-Triggered" Drug Release, Macromolecules, 44 (2011) 1327-1334.
[21] S. Yamamoto, K. Nishimura, K. Morita, S. Kanemitsu, Y. Nishida, T. Morimoto, T. Aoi, A. Tamura, T. Maruyama, Microenvironment pH-Induced Selective Cell Death for Potential Cancer Therapy Using Nanofibrous Self-Assembly of a Peptide Amphiphile, Biomacromolecules, 22 (2021) 2524-2531.
[22] R. Montanari, Cold chain tracking: a managerial perspective, Trends Food Sci. Technol., 19 (2008) 425-431.
[23] J.Y. Wu, H.I. Hsiao, Food quality and safety risk diagnosis in the food cold chain through failure mode and effect analysis, Food Control, 120 (2021).
[24] Y. Wang, J. Zhang, X.Y. Guan, M.Z. Xu, Z. Wang, H.Z. Wang, Collaborative multiple centers fresh logistics distribution network optimization with resource sharing and temperature control constraints, Expert Syst. Appl., 165 (2021).